environments

Article

Sustainable Co-Management of Acid Mine Drainage with Struvite Synthesis Effluent: Pragmatic Synergies in Circular Economy

Vhahangwele Masindi [1,2,3,*], Ryneth Mbhele [3] and Spyros Foteinis [3,4,*]

[1] Magalies Water, Scientific Services, Research & Development Division, Erf 3475, Stoffberg Street, Brits 0250, South Africa
[2] Department of Environmental Sciences, College of Agriculture and Environmental Sciences, University of South Africa (UNISA), Florida 1710, South Africa
[3] Council for Scientific and Industrial Research (CSIR), Smart Places, Water Centre, Pretoria 0001, South Africa; rmbhele@csir.co.za
[4] Research Centre for Carbon Solutions, School of Engineering and Physical Sciences, Heriot-Watt University, Edinburgh EH14 4AS, UK
* Correspondence: vhahangwelem@magalieswater.co.za (V.M.); s.foteinis@hw.ac.uk (S.F.); Tel.: +27-01-2381-6602 (V.M.)

Abstract: Herein, the alkaline supernatant of a struvite recovery system from municipal wastewater was successfully co-managed with acid mine drainage (AMD). Various ratios (v/v) of AMD to struvite supernatant were examined, and the quality of the passively co-treated effluent and of the generated sludge were examined using state-of-the-art analytical techniques including ICP-OES, FE-SEM/FIB/EDX, XRD, XRF, and FTIR. The optimum ratio was 1:9, where metals and sulphate were largely removed from AMD, i.e., from higher to lower score Fe (~100%) ≥ Pb (~100%) ≥ Ni (99.6%) ≥ Cu (96%) ≥ As (95%) ≥ Al (93.7%) ≥ Zn (92.7%) > Ca (90.5%) > Mn (90%) ≥ Cr (90%) > sulphate (88%) > Mg (85.7%), thus implying that opportunities for mineral recovery could be pursued. The pH of the final effluent was regulated to acceptable discharge levels, i.e., 6.5 instead of 2.2 (AMD) and 10.5 (struvite supernatant), while a notable reduction in the electrical conductivity further implied the attenuation of contaminants. Overall, results suggest the feasibility of the passive co-treatment of these wastewater matrices and that opportunities for direct scaling up exist (e.g., using waste stabilization ponds). Furthermore, apart from the initial recovery of struvite from municipal wastewater, metals could also be recovered from AMD and water could be reclaimed, therefore introducing circular economy and zero liquid discharge in wastewater treatment and management.

Keywords: magnesium ammonium phosphate (MAP); zero liquid discharge (ZLD) process; sustainable water and wastewater treatment; waste valorization and beneficiation; phosphate and ammonia recovery-recycling; UN SDG 6: clean water and sanitation

Citation: Masindi, V.; Mbhele, R.; Foteinis, S. Sustainable Co-Management of Acid Mine Drainage with Struvite Synthesis Effluent: Pragmatic Synergies in Circular Economy. *Environments* **2023**, *10*, 60. https://doi.org/10.3390/environments10040060

Academic Editor: Daisuke Minakata

Received: 13 February 2023
Revised: 18 March 2023
Accepted: 24 March 2023
Published: 4 April 2023

1. Introduction

The problem of the dwindling phosphate rock reserves has brought forward the need for alternative phosphorus (P) sources, with the recovery of struvite (also known as magnesium ammonium phosphate (MAP)) from P-rich wastewaters, notably municipal wastewater (MWW), having emerged as a promising alternative [1,2]. Nutrients recovery from wastewater can also offset the environmental impact of the treatment process; while water could also be reclaimed, thus introducing zero-liquid discharge (ZLD) and a circular economy in wastewater management [3,4]. However, a main concern is the highly alkaline effluent (supernatant) that is generated during struvite synthesis and recovery, which requires proper management and disposal [5,6]. Nonetheless, the high alkalinity itself can be used for the neutralization and (co-)treatment of acidic effluents such as acid mine drainage (AMD) [6].

Specifically, AMD comprise an acidic matrix that is rich in dissolved chemical species, primarily sulphate and metals such as aluminium (Al), iron (Fe), manganese (Mn), zinc (Zn), copper (Cu), nickel (Ni), lead (Pb), calcium (Ca), magnesium (Mg), and in some cases rare earth elements [7–9]. As such, the release of untreated AMD into receiving ecosystems can cause toxic and hazardous effects since it can lead to mutagenic, teratogenic, and carcinogenic impacts on living organisms [10]. The reason behind the high dissolution of metals in AMD is its high acidity, with pH levels reaching even lower than 2 in some cases [7,11]. Traditionally, AMD decontamination has been achieved using active and/or passive treatment technologies [12–14]. Active treatment typically includes neutralization (e.g., lime treatment), filtration (e.g., reverse osmosis), adsorption (e.g., zeolites), and ion exchange (e.g., resins), whereas passive treatment typically includes bioremediation (e.g., bioreactors), permeable reactive barriers (e.g., limestone gravels), evaporation ponds, wetlands, and co-disposal with other wastewater streams [8,10,13]. In general, active treatment is more effective in terms of residence time and contaminants removal, but passive treatment requires less space, infrastructure, materials, and energy inputs and does not produce a highly mineralized sludge that needs to be properly managed [10]. However, the recently introduced concepts of circular economy and ZLD in wastewater management necessitate the introduction of wastewater beneficiation, valorization, and reuse, with the co-treatment of different wastewater matrices being promising in this regard [6,15,16]. Specifically, the co-treatment of MWW with AMD has been found promising due to the P(MWW)—metals (AMD) scavenging mechanism [17]. Not only this, but struvite that has been recovered from MWW has also been used for the treatment of AMD [5]. However, the use of the supernatant of struvite synthesis, which is a P-depleted alkaline effluent, has not been examined for co-treatment with AMD. In previous research, the passive (no active mixing) co-treatment of a different P-depleted MWW matrix, i.e., supernatant from a calcium phosphate recovery system, with AMD was examined and found promising [6]. This system was based on the use of calcium hydroxide ($Ca(OH)_2$) to synthesize and recover calcium phosphate from MWW, thus producing a Ca-rich and alkaline effluent. In struvite recovery systems, magnesium oxide (MgO) is typically used, which again produces an alkaline effluent, but in this case the pH is typically lower, and the Mg content is much higher than the Ca content. As such, this effluent could also have potential for co-management with AMD.

For this reason, the passive co-treatment of struvite synthesis supernatant with MWW is examined herein. Focus is placed on both the quality of the co-treated effluent and on the characterization of the produced sludge (product sludge thereafter). Water quality is an important aspect, since this will define if the co-treated effluent can be released to the environment and if it is possible, with further polishing, to reclaim water. The latter is of particular importance for water-scarce countries such as South Africa, the case study herein. Regarding the product sludge, the main focus here was to identify if valuable minerals were synthesized during the interaction of struvite supernatant with MWW. Therefore, the target of this study is twofold. First and foremost, to examine the feasibility of the passive co-management of these two wastewater matrices and, second, to identify opportunities for the recovery of valuable minerals from AMD (beneficiation) and for water reclamation. The latter could lead to the introduction of circular economy and ZLD in the management of these wastewater matrices. This is of major importance for the developing world, where infrastructure is underdeveloped or undeveloped and water is scarce, thus also fostering the United Nations Sustainable Development Goals (SDGs) and particularly goal no 6: Clean Water and Sanitation.

2. Materials and Methods

2.1. Sample Collection

The struvite synthesis supernatant, or simply the struvite supernatant, was acquired from a struvite recovery system, which recovers P from MWW in the South African setting and has been extensively covered in previous research [4,18,19]. For its collection, the

grab sampling technique was selected over composite sampling, owing to the fact that the effluent characteristics did not greatly fluctuate over time. For the removal of debris and suspended solids, the collected MWW was passed through Macherey-Nagel™ filter papers (MN 615. Ø125 mm), and the preliminary treated effluent was then stored in high-density polyethylene (HDPE) containers in a cool and dark place. The AMD was collected from a coal handling facility, where leachates seep from the toe of a large coal heap to a small evaporation pond. As such, the AMD was concentrated and fully oxidized due to exposure to air and water. The coal preparation plant is sited in the vicinity of a coal mine, i.e., in Mpumalanga province, South Africa. Similarly, the raw AMD was filtered using Macherey-Nagel™ filter papers (MN 615. Ø125 mm), moved to HDPE containers, and stored in a cool and dark place until utilization. Heedworthy, the co-treatment experiments were carried out soon after sampling to prevent aging of the samples and secondary reactions. After the interaction of the AMD with the struvite supernatant, the mixture was left to equilibrate and for the produced to precipitate. The product sludge was then collected using perforated Macherey-Nagel filter papers and dried, so that it could be characterized and further examined. All experiments and measurements were carried out in an ISO/IEC 17025:2017 accredited laboratory, following standard methods and procedures.

2.2. Methods for Sample Characterization

To fulfill the objectives of this study, the following analytical pieces of equipment were employed for the characterization of the aqueous (struvite supernatant, AMD, and co-treated effluent) and solid (product sludge) samples. Specifically, for the aqueous samples, Hanna's HI-9828 multi-parameter water quality instrument was used to measure the pH and electrical conductivity (EC). Furthermore, macronutrients, metals, and non-metals were measured using the Thermo Scientific™ Gallery™ Plus (discrete analyzer) (Waltham, MA, USA) and inductively coupled optical emission spectroscopy (ICP-OES) (Agilent, 5110 ICP-OES, Santa Clara, CA, USA).

For the characterization of the product sludge, i.e., the sludge that is produced from the interaction of AMD with the struvite supernatant, different analytical instruments were employed to identify its elemental, mineralogical, and microstructural properties. Specifically, a high-resolution (HR) field emission scanning electron microscope (FESEM), coupled with focused ion beam (FIB) (Cobra column) and energy-dispersive X-ray spectroscopy (EDX) (i.e., the Carl Zeiss AURIGA® Series modular Cross-Beam® workstation, Jena, Germany), was used for elemental mapping, elemental composition, spot analysis, and microstructural characteristics identification. The functional groups were detected by means of Fourier transform infrared spectroscopy (FTIR) (Perkin Elmer Spectrum 100 fitted with an attenuated total reflectance (ATR) accessory, Waltham, MA, USA). The elemental composition was also measured using X-ray fluorescence (XRF) (Thermo Scientific™ ARL™ PERFORM'X using the lithium-borate fusion technique and coupled with the UniQuant software (V 5.57) for standardless analyses). Finally, the mineralogical characteristics were ascertained using X-ray diffraction (XRD) (PANalytical X'Pert Pro multipurpose X-ray diffractometer (Fe-filtered Co-Kα anode (λ = 1.789 Å) in theta configuration with variable divergence).

2.3. Co-Treatment Experimental Setup

In previous research, it was identified that if (alkaline) wastewater was allowed ample time to equilibrate with AMD under ambient conditions (i.e., room temperature and without controlling the pH of the samples), then the main factor affecting the attenuation of the different contaminants was the liquid-to-liquid (L:L) ratio [6,15]. For this reason, different AMD to struvite supernatant ratios were examined, i.e., 1:5, 1:6, 1:7, 1:8, and 1:9. Regarding the experimental setup, all experiments were conducted at bench scale using borosilicate glass beakers. Specifically, the AMD volume was fixed at 10 mL, and varying volumes of the struvite supernatant, i.e., 50, 60, 70, 80, and 90 mL, were added into individual beakers and left to react for 12 h. The equilibrated samples were then collected

for further analyses, and the results are presented below. It should be noted that the initial pH of AMD was 2.2 and that of the struvite supernatant was 10.5.

2.4. Statistical Analyses

For quality control, all experiments were performed in triplicate. The aqueous samples were then characterized for each experimental run, and the corresponding results are reported as mean values. It should be noted that the measurements for the aqueous samples yielded low standard deviations, i.e., the average amount of variability for each examined parameter was low. The overall low standard deviation values imply that similar results were obtained in each of the three experimental runs and, therefore, that the collected solid material (product sludge) had similar properties in each experimental run. Therefore, the analyses for the solid sample (product sludge) were not performed in triplicate.

3. Results and Discussion

3.1. Effect of Liquid-to-Liquid Ratio

The results for the effect of the L:L ratio (AMD to struvite supernatant) on the co-treatment efficiency are shown in Figure 1. As can be seen, the contaminants percentage removal increases with decreasing L:L ratios, i.e., when AMD is diluted in higher struvite supernatant volumes, with the optimal percentage removals observed at the lower end of the examined range, i.e., 1:9. For example, at this L:L ratio, EC decreases by 88% due to the overall reduction of dissolved chemical species in both wastewater matrices, whereas Mg and Ca are reduced by 85.7% and 90.5%, respectively (Figure 1a). Furthermore, sulphate (Figure 1b) also decreases along with Ca (Figure 1a), and this could denote the possible formation of gypsum. The pH of the co-treated effluent was also observed to increase with decreasing L:L ratios, e.g., going from 3 at the 1:5 ratio to 6.5 at the 1:9 ratio (Figure 1b). In more detail, at the two lower examined ratios, i.e., 1:8 and 1:9, the pH of the co-treated effluent was 6 and 6.5, respectively, from the initial pH of 2.2 for the AMD and 10.5 for the struvite supernatant, and therefore is within the South African limits for discharge to the environment [20]. Furthermore, with reference to Figure 1b, it appears that the 6.5 pH (1:9 ratio) is also sufficient for the effective removal of different contaminants contained in these two wastewater streams (Figure 1). Therefore, the obtained results reflect a significant removal of contaminants with decreasing L:L ratios, with the optimal ratio being 1:9 (i.e., 10 mL of AMD per 90 mL of struvite supernatant). At this ratio, the removal of the different contaminants exhibits the following pattern: Fe $\geq$ Pb $\geq$ Ni $\geq$ Cu $\geq$ arsenic (As) $\geq$ Al $\geq$ Zn > Ca > Mn $\geq$ chromium (Cr) > sulphate > Mg (Figure 1). In light of that, the co-management of AMD with struvite supernatant appears as a promising solution for the effective and, most likely, sustainable management of both effluents.

3.2. Co-Management at Optimal Conditions

With reference to the aforementioned results, the optimal L:L ratio for the treatment of the real AMD with the struvite supernatant was 1:9. Therefore, the co-treatment experiments were repeated at this ratio, but this time using much larger volumes (1 L containers) to assess whether the co-treatment volume affects the results and also to be able to collect a usable amount of product sludge for characterization. Results are reported in Table 1.

Similar to the L:L ratio results (Section 3.1), the passive co-treatment of the real AMD with struvite supernatant at higher volumes was found to significantly attenuate contaminants from both wastewater matrices. Specifically, the AMD was highly acidic and rich in Fe and sulphate in addition to other chemical species, and this could be traced back to the parent mineral being oxidized, i.e., pyrite. Contrariwise, the struvite supernatant contained minute levels of P, hence an insignificant concentration of orthophosphate, while its high pH value suggests that this effluent is alkaline. In addition, the levels of Mg and Ca in struvite supernatant were very low, and this could be explained by the reaction between phosphate, ammonia, and Mg in MWW, which led to their removal as struvite. The correction of the pH from 2.2 and 10.5 in the AMD and the struvite supernatant, respectively, to

6.5 in the co-treated effluent can be explained by the neutralization of the acidity contained in AMD and the alkalinity contained in struvite supernatant. Furthermore, the percentage removals are in agreement with the ones of the aforementioned results (Section 3.1), with the percentage removals being, from higher to lower score, Fe (~100% removal) ≥ Pb (~100%) ≥ Ni (99.6%) ≥ Cu (96%) ≥ As (95%) ≥ Al (93.7%) ≥ Zn (92.7%) > Ca (90.5%) > Mn (90%) ≥ Cr (90%) > sulphate (88%) > Mg (85.7%) (Table 1). In particular, the principal mechanisms that govern the removal of contaminants are dilution, precipitation, co-precipitation, adsorption, co-adsorption, and complexation. For example, the large reduction in EC can be mainly traced back to the (co)precipitation of metals and sulphate, e.g., as metal (hydr)oxides and gypsum, and dilution. When the results are compared with the ones for the passive co-treatment of AMD with calcium phosphate supernatant [6], it appears that the latter achieved higher percentage efficiencies in contaminants removal for the same L:L ratio (1:9). This was expected since $Ca(OH)_2$, which is more alkaline than MgO, is used in calcium phosphate recovery systems from MWW. As such, the pH of the calcium phosphate effluent is higher than that of the struvite synthesis effluent (11.5 [6] instead of 10.5 here), and this is more beneficial for metals and contaminants precipitation when using the same L:L ratio. Furthermore, even though this passive co-treatment approach is not as efficient as typical AMD treatment technologies [10], is not material and energy intensive, complex, or costly, while another wastewater matrix (struvite supernatant) is also managed. Therefore, this process can introduce more sustainable treatment approaches for both AMD and struvite supernatant.

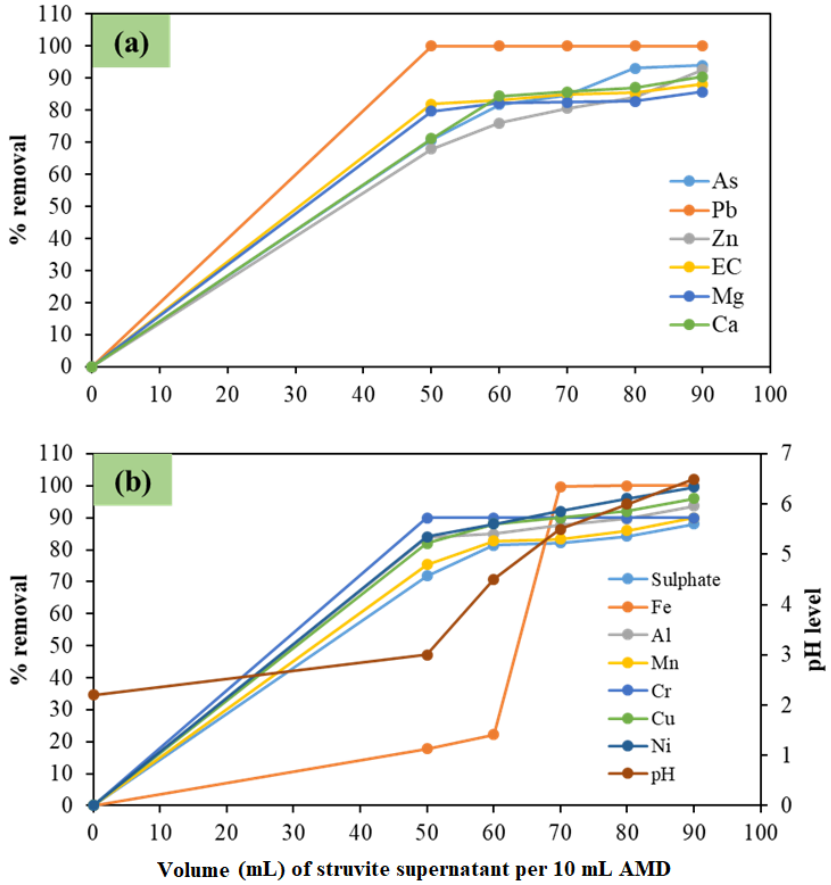

Figure 1. Changes in the pH and contaminants percentage (%) removal, i.e., (**a**) As, Pb, Zn, EC, Mg, and Ca; and (**b**) sulphate, Fe, Al, Mn, Cr, Cu, Ni, and pH, when using different AMD to struvite supernatant ratios. Conditions: 10 mL of AMD and varying mL of struvite -supernatant, room temperature, and 12 h equilibrium time.

Table 1. Outcomes for the co-treatment of AMD with struvite supernatant at 1:9 ratio, 12 h equilibrium time, and room temperature (n = 3 but results were reported as mean value).

Parameters	AMD	Struvite Supernatant	Co-Treated Effluent
Sulphate (mg/L)	18000 ± 2.61	22 ± 0.69	2153 ± 1.44
Total iron (mg/L)	4500 ± 0.31	7 ± 0.05	0.1 ± 0.00
Total aluminium (mg/L)	800 ± 0.01	0.01 ± 0.00	50.3 ± 0.13
Total manganese (mg/L)	150 ± 0.50	0.19 ± 0.92	15 ± 0.13
Total chromium (mg/L)	0.1 ± 0.00	0.06 ± 0.22	0.01 ± 0.00
Total copper (mg/L)	0.5 ± 0.00	0.03 ± 0.02	0.02 ± 0.01
Total nickel (mg/L)	2.5 ± 0.02	0.07 ± 0.13	0.01 ± 0.00
Total arsenic (mg/L)	0.1 ± 0.00	0.05 ± 0.01	0.005 ± 0.09
Total lead (mg/L)	0.35 ± 0.58	0.05 ± 0.05	0.00001 ± 0.06
pH (logarithmic units)	2.5 ± 0.01	10.5 ± 0.01	6.5 ± 0.07
Electrical conductivity (mS/cm)	2800 ± 0.02	89 ± 0.05	458 ± 1.33
Total zinc (mg/L)	15 ± 0.08	0.02 ± 0.01	1.1 ± 0.04
Orthophosphate (mg/L)	0.05 ± 0.19	0.7 ± 0.12	0.00001 ± 0.05
Ammonia (mg/L)	5.7 ± 0.23	28 ± 1.55	22.7 ± 0.75
Total calcium (mg/L)	576 ± 2.1	8.9 ± 0.75	55 ± 0.83
Total magnesium (mg/L)	771 ± 1.13	68 ± 0.99	110 ± 0.51

Overall, it can be claimed that the co-treatment of AMD with struvite supernatant, a P-depleted MWW matrix, can be a promising intervention for the effective and sustainable management of both wastewater streams. However, much higher volumes of struvite supernatant are required compared to AMD. Therefore, for the processes to become applicable at large scales and under real-world conditions, where AMD volumes can be significantly larger than the ones of struvite supernatant, the pH of the AMD-struvite supernatant mixture can be controlled using low-cost and readily available chemical reagents such as lime or caustic soda (NaOH). Furthermore, even though the pH of the final (co-treated) effluent was corrected, this was not fit for release into the receiving environment since, among others, sulphate contamination persisted (Table 1). For this reason, the residual sulphate and the remaining contaminants should be removed using a polishing technology (e.g., membrane filtration), and this could render this effluent fit for release to the environment as well as other defined uses such as for agricultural use or even for drinking water. It should be noted that water reclamation is of major importance for water scarce countries that are also affected by AMD, such as South Africa. Therefore, this approach could also generate revenue and offset the running costs of the process, possibly leading to avoided emissions and improving its environmental sustainability, thus making the process self-sustainable and environmentally friendly.

3.3. Product Sludge Characterization

In order to supplement the co-treated effluent results (Sections 3.1 and 3.2), the sludge that was generated from the interaction of the AMD with the struvite supernatant (product sludge) was also characterized, and results are reported below.

3.3.1. Elemental Analysis Using X-ray Fluorescence

Quantitative information on the elements that are embedded in the product sludge was obtained by the XRF technique. It was identified that the chemical composition of the product sludge was dominated by the metals/elements that were dominant in the AMD, i.e., sulphur (S) and Fe, followed by Ca, Mg, Al, and Si, and traces of other elements (Table 2). The observed concentrations trace back to the corresponding concentrations of these elements in both wastewater matrices and mainly to AMD which was rich in metals and sulphate. Furthermore, the pH of the co-treated effluent (6.5) also affected the precipitation potential of different metals/elements. For example, in AMD, Fe precipitates best at pH 3.5 to 4 and Al at pH 6 to 7 [21–23]. Therefore, Fe was fully removed from the co-treated effluent and migrated to the product sludge, while this was not the case for Al,

as reflected in its concentration in the co-treated effluent (Table 1) and in the product sludge (Table 2). The high S and Ca values could also possibly suggest gypsum formation, and the values for Fe, Al, and Si could suggest the formation of metal hydroxides, including Si-based minerals among others, in the product sludge. Overall, the XRF results denote that the product sludge is a sink for the contaminants that were embedded in the AMD and the struvite supernatant, and this highlights the high efficiency of the co-treatment process in contaminants removal.

Table 2. The elemental composition (wt.%) of the product sludge as determined by the XRF technique.

Element/Metal	Mass Fraction (%)	Element/Metal	Mass Fraction (%)
SiO_2	1.82	MnO	0.65
Al_2O_3	3.89	NiO	<0.01
MgO	12.12	CuO	<0.01
Na_2O	0.37	ZrO_2	<0.01
P_2O_5	0.09	S	10.33
Fe_2O_3	29.43	Cl	<0.01
K_2O	0.03	Co_3O_4	0.02
CaO	13.77	ZnO	0.09
TiO_2	<0.01	Ag_2O	0.19
V_2O_5	<0.01	LOI	26.53
Cr_2O_3	<0.01	TOTAL	99.91

3.3.2. Elemental Analysis Using Energy-Dispersive X-ray Spectroscopy

The elemental composition of the product sludge was also measured using SEM-EDX, and the respective results are shown in Figure 2. Specifically, EDX revealed the predominance of carbon (C), oxygen (O), Ca, S, Fe, and Mg amongst traces of Al, chlorine (Cl), potassium (K), and silicon (Si) in the product sludge surface. It should be noted that O and C, and in general, elements with atomic number lower than 11, can be detected by EDX but cannot be reliably quantified and therefore are not considered herein. Furthermore, the presence of C is linked to the coating material that was used during EDX analysis and not to the sample itself. However, the presence of O in product sludge could suggest that metals have precipitated as (hydr)oxides, e.g., Fe and Al hydroxides. The presence of Ca and S denotes the possible formation of gypsum or any of its species, while the presence of Mg, Fe, and Si could also be linked to magnesium iron silicate hydroxide formation. The obtained results corroborate the XRF results (Section 3.3.1). They further highlight that contaminants from both matrices are removed and migrate to the product sludge, hence also correlating with the results for the co-treated effluent (Sections 3.1 and 3.2).

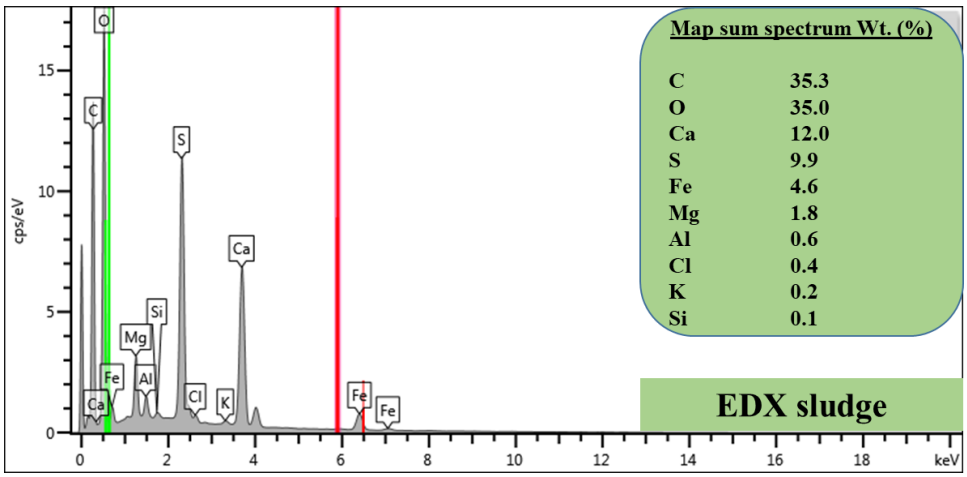

Figure 2. The elemental characteristics of the product sludge as quantified using the EDX.

3.3.3. Functional Groups and Mineral Analysis

The functional groups of the product sludge were identified by FTIR, whereas the mineralogical characteristics were determined by XRD. Results are presented in Figure 3. Specifically, the FTIR spectrum graph shown in Figure 3a highlight the peaks that correspond to the different species contained in the product sludge. FE-O stretching and bending modes at 560, 600, 950, and 3500 cm^{-1} imply the formation of hydrated Fe-based minerals [24], such as hydroxides, as determined by EDX. The sulphate stretching was observed between 1050 and 1600 cm^{-1}, as has been highlighted elsewhere [25], and this could suggest the presence of gypsum in the product mineral, while the OH group verified the presence of hydrated minerals such as Fe hydroxide, Al hydroxide, and oxyhydrosulphate. The carbonate could originate from the parent material (magnesite) of MgO and/or ingression of atmospheric carbon dioxide (CO_2) into MgO before use for struvite recovery from MWW or thereafter. Findings from this study corroborate findings from previous research, where geochemical modeling (PHREEQC) had also been employed [5,6,15,22,26]. Moreover, the outcomes are consistent with what was identified by XRF and EDX techniques. The findings on the mineralogical characteristics of the product sludge are summarized in Figure 3b, where it is shown that basanite, a form of gypsum (calcium sulphate), is the principal crystalline mineral in the product sludge. Furthermore, the noisy peaks identified in the diffractogram insinuate the potential existence of amorphous phases. These cannot be determined by XRD since the phases should be crystalline. The XRD results complement the results that were presented above. Overall, a relationship between the results for the co-treated effluent and the product sludge becomes apparent and demonstrates the interchange of chemical species and their fate in the product sludge after the co-treatment of AMD with struvite supernatant.

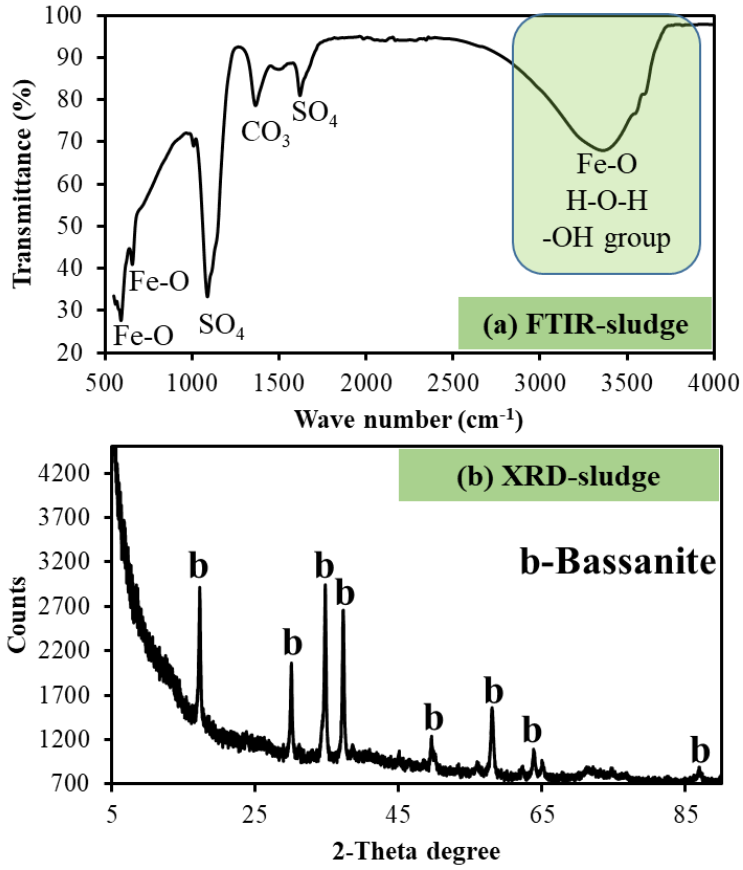

Figure 3. The (**a**) functional groups and (**b**) mineralogical characteristics of the product sludge, where lower-case "b" in the diffractogram stand for "Bassanite".

3.3.4. Morphological and Microstructural Characteristics

Morphological and microstructural analyses were performed by means of FIB-SEM. High-resolution images were obtained, which shed light on the product sludge's precise characteristics. Specifically, as shown in Figure 4, the product sludge consisted of heterogeneous particles, mainly rod-like structures staked together in addition to spherical-like structures. Different magnifications, in the range of 2 µm to 100 nm, were employed, and these gave similar results. This implies that the product sludge is uniform and homogenous in nature. Overall, the obtained results corroborate the results of previous research, which reported gypsum to present a rod-like structure and Al-, Fe-, Mg-, K-, and Mn-based minerals a spherical structure [6].

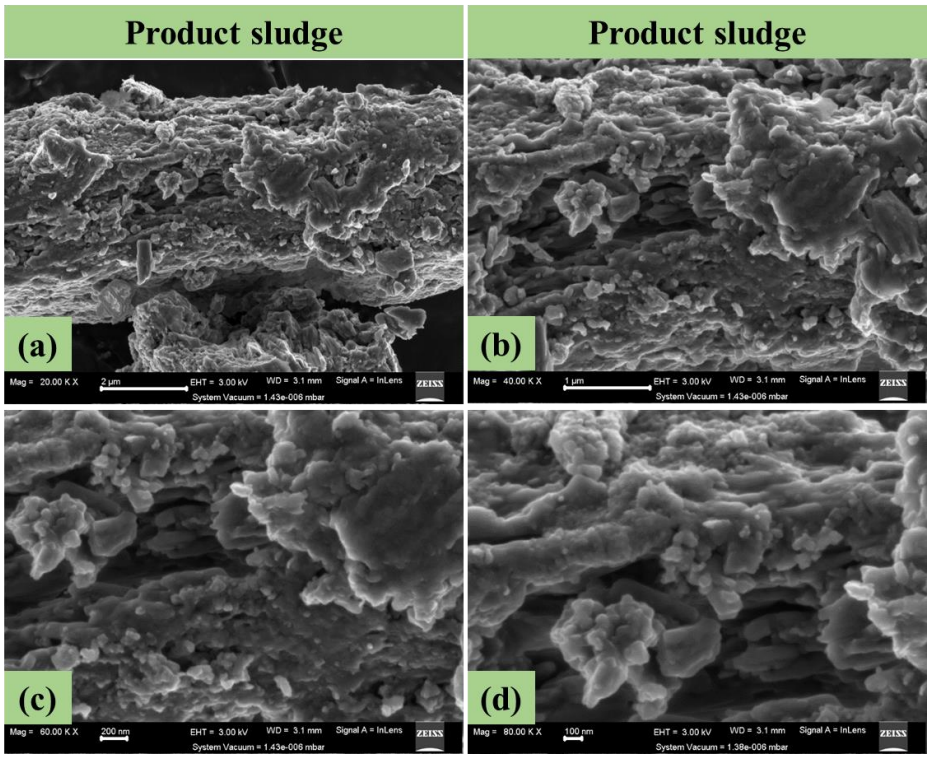

Figure 4. Microstructural and morphological properties of the product sludge at (**a**) 2 µm, (**b**) 1 µm, (**c**) 200 nm, and (**d**) 100 nm magnification.

3.3.5. Energy Dispersive X-ray Spectroscopy Elemental Mapping

The SEM-EDX micrograph of the product sludge and elemental mapping of S, O, Ca, Fe, Al, Mg, K, Cl, and Si are reported in Figure 5. The EDX elemental maps can provide qualitative information based on the color intensity of the respective element, with higher intensities suggesting higher elemental concentration. Therefore, Figure 5 suggests an abundance of S, O, Ca, and Fe and lower concentrations of Al, Mg, K, Cl, and Si in the product sludge. This is also in agreement with the peaks of these elements that were identified in Figure 2 using SEM-EDX. Furthermore, as discussed above, S, and Ca identified in the rod-like structures possibly denote gypsum formation [15,27], while the concurrent presence of O suggests that this material is hydrated, i.e., basanite has been formed (Section 3.3.3). Other particles, which were mainly dominated by spherical-like structures, most likely represent the formation of Fe-based minerals in the product sludge, which include in their matrix the identified metal and non-metal elements (Al, Mg, K, Si, and Cl). On the other hand, the overlay of these elements with O suggests that metal (hydr)oxides might have been formed. Therefore, the SEM-EDX results are in agreement with the results of the other analytical techniques that were discussed above.

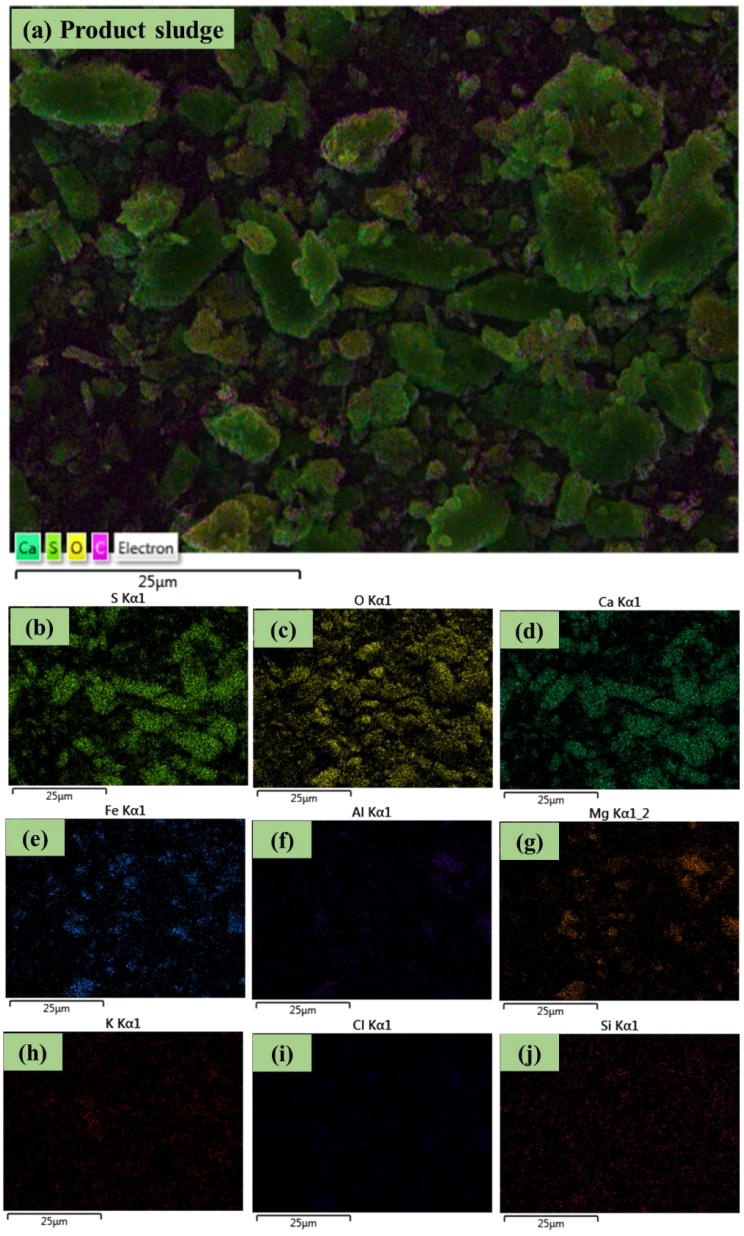

Figure 5. (**a**) The SEM-EDX micrograph of the product sludge and the elemental mapping of (**b**) S, (**c**) O, (**d**) Ca, (**e**) Fe, (**f**) Al, (**g**) Mg, (**h**) K, (**i**) Cl, and (**j**) Si.

3.3.6. Spot Analysis

In order to further corroborate the results obtained from the aforementioned analytical techniques, spot elemental analysis was also pursued using HR-SEM-EDX. The morphology and EDX profiling of the product sludge, including composition analysis, are presented in Figure 6. Specifically, the predominant morphological properties of the product sludge were rod-like structures of various widths and lengths, denoting the possible formation of gypsum [6]. These were sandwiched between spherical particles. Furthermore, a few spherical and octagonal-like structures were also observed, which denote the formation of Fe-based minerals. This was expected, since the co-treated effluent results (Section 3.2) highlighted the removal of Fe and S, as the main elements, from the AMD—struvite supernatant mixture. Finally, as expected, the elemental and structural details of the surface of the product sludge (Figure 6) are in agreement with what has been discussed above since they revealed S, Ca, and O in the rod-like structures, suggesting the possible formation of

hydrated gypsum, and spherical-like structures, mainly containing Fe and O, suggesting the formation of Fe-based metal hydroxides.

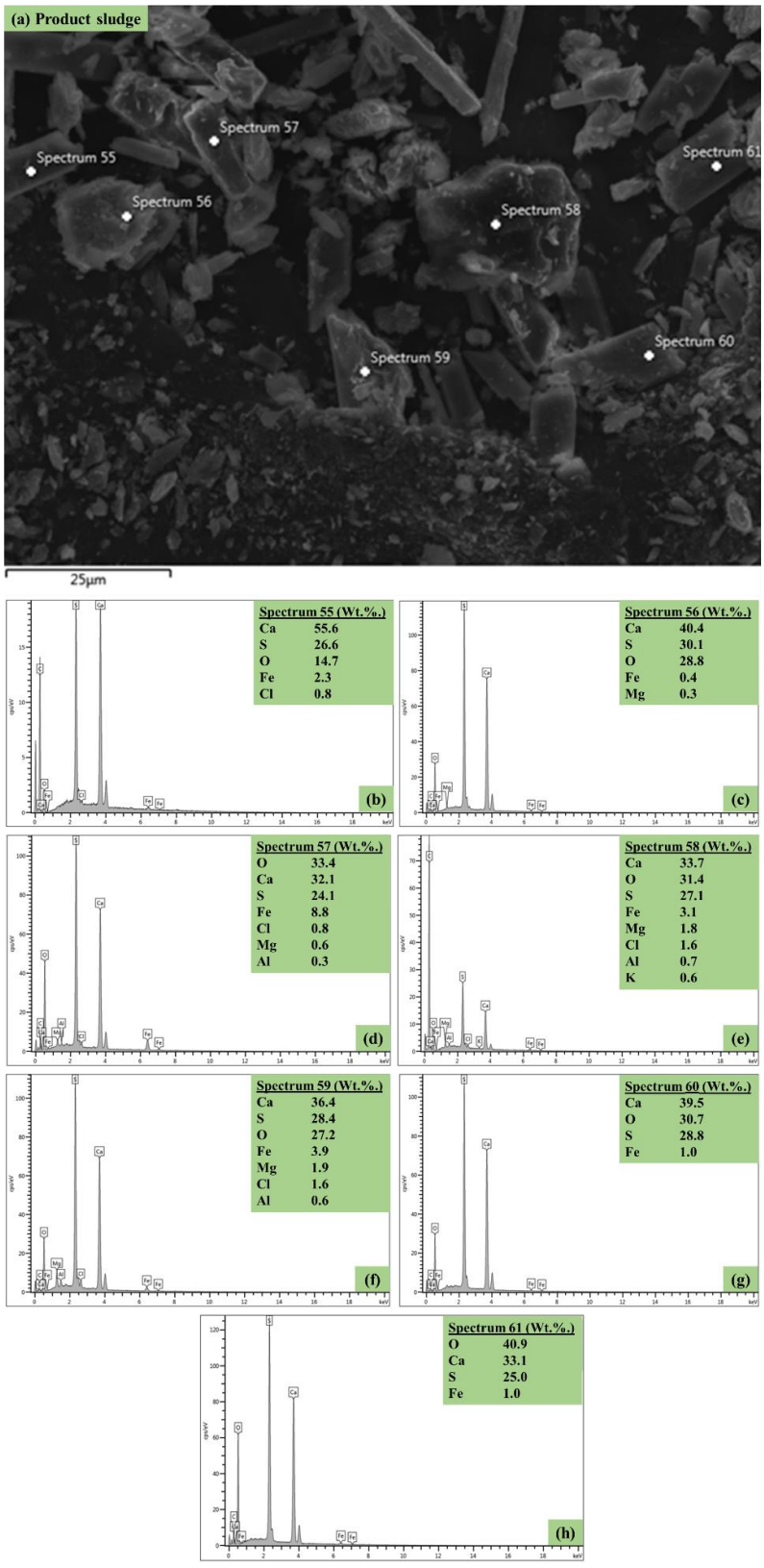

Figure 6. (**a**–**h**)**:** The HR-SEM-EDX morphological results showing: (**a**) the spot analysis image of the product sludge, and (**b**–**h**) the respective spot elemental compositions.

Overall, results highlighted that important and valuable minerals are contained in the product sludge, raising the possibility of their recovery. As is the case with the opportunities for reclaiming water from the co-treated effluent, the minerals that could possibly be recovered from the product sludge can provide a new revenue, thus helping to make the co-treatment process self-sustainable. This could also reduce the overall environmental impact of the process through avoided emissions, i.e., the recovered minerals could be used in industrial processes instead of virgin minerals. Therefore, results highlight that pragmatic synergies can be achieved when different wastewater matrices are co-managed and that opportunities for introducing the circular economy and ZLD to wastewater management are available. Finally, as is the case with every technology, the scaling up of this co-treatment approach may face a wide spectrum of difficulties, including spatial restrictions, e.g., challenges in collecting and transporting the wastewaters to the same treatment facility, and problems in the mixing conditions in industrial-scale systems. Nonetheless, for the sustainable scaling up of this technology, opportunities for using existing technology could also be explored. For example, in this bench-scale study, gravity filtration was employed as the mode of solids/liquid separation. However, in upscaled systems, drying pans or filter presses could be used as the mode of sludge/liquid separation.

4. Conclusions

The sustainable and effective co-treatment of real acid mine drainage (AMD) with struvite synthesis supernatant was highlighted herein, also identifying that pragmatic synergies can be successfully pursued through their co-management. The treatment was passive for a period of 12 h to enhance reactivity. Findings from this study demonstrated the following performance efficacy, from higher to lower score: Fe $\geq$ Pb $\geq$ Ni $\geq$ Cu $\geq$ As $\geq$ Al $\geq$ Zn > Ca > Mn $\geq$ Cr > sulphate > Mg. For the 1:9 L:L (AMD to struvite supernatant) ratio, the respective removal efficiencies were ~100% $\geq$ ~100% > 99.6% > 96% > 95% > 93.7% > 92.7% > 90.5% > 90% $\geq$ 90% > 88% > 85.7%.

The co-removal of contaminants was primarily influenced by the reactions between the different chemical species contained in these two effluents, leading to their removal as (hydr)oxides, amongst others. Furthermore, dilution, as well as (co)adsorption, complexation, crystallization, and (co)precipitation, were observed as the main mechanisms in the attenuation of contaminants. The fate of chemical species was determined using a variety of state-of-the-art analytical techniques, and the product sludge was determined to be rich in gypsum and Fe-based minerals, among traces of other chemical species.

In light of the obtained results, this study will go a long way in introducing sustainable alternatives for the effective management of struvite synthesis supernatant and drainage from coal and gold mining activities, while at the same time opening up opportunities for water reclamation and minerals recovery. Future research should examine avenues for water reclamation (e.g., using lime to remove residual sulphate and then membrane filtration or other polishing technologies) and the feasibility of recovering minerals from the product sludge, i.e., exploring beneficiation opportunities.

Author Contributions: V.M.: conceptualization, validation, formal analysis, investigation, resources, data curation, writing—original draft, writing—review and editing, visualization, funding acquisition, and project administration; R.M.: conceptualization, validation, formal analysis, investigation, data curation, visualization, and writing—review and editing; and S.F.: conceptualization, validation, formal analysis, investigation, visualization, and writing—review and editing. All authors have read and agreed to the published version of the manuscript.

Funding: This research received no external funding.

Data Availability Statement: Data are available upon request.

Acknowledgments: The authors would like to thank Magalies Water, the University of South Africa, and the Council for Scientific and Industrial Research (CSIR). Furthermore, we would like to thank the staff of the coal mine and the municipal wastewater treatment facilities for their help during sampling and the lab technicians who worked to obtain the presented results.

Conflicts of Interest: The authors declare no conflict of interest.

References

1. Rahman, M.M.; Salleh, M.A.M.; Rashid, U.; Ahsan, A.; Hossain, M.M.; Ra, C.S. Production of slow release crystal fertilizer from wastewaters through struvite crystallization—A review. *Arab. J. Chem.* **2014**, *7*, 139–155. [CrossRef]
2. Peng, L.; Dai, H.; Wu, Y.; Peng, Y.; Lu, X. A comprehensive review of phosphorus recovery from wastewater by crystallization processes. *Chemosphere* **2018**, *197*, 768–781. [CrossRef]
3. Sena, M.; Hicks, A. Life cycle assessment review of struvite precipitation in wastewater treatment. *Resour. Conserv. Recycl.* **2018**, *139*, 194–204. [CrossRef]
4. Mavhungu, A.; Masindi, V.; Foteinis, S.; Mbaya, R.; Tekere, M.; Kortidis, I.; Chatzisymeon, E. Advocating circular economy in wastewater treatment: Struvite formation and drinking water reclamation from real municipal effluents. *J. Environ. Chem. Eng.* **2020**, *8*, 103957. [CrossRef]
5. Masindi, V.; Fosso-Kankeu, E.; Mamakoa, E.; Nkambule, T.T.I.; Mamba, B.B.; Naushad, M.; Pandey, S. Emerging remediation potentiality of struvite developed from municipal wastewater for the treatment of acid mine drainage. *Environ. Res.* **2022**, *210*, 112944. [CrossRef]
6. Masindi, V.; Shabalala, A.; Foteinis, S. Passive co-treatment of phosphorus-depleted municipal wastewater with acid mine drainage: Towards sustainable wastewater management systems. *J. Environ. Manag.* **2022**, *324*, 116399. [CrossRef] [PubMed]
7. Naidu, G.; Ryu, S.; Thiruvenkatachari, R.; Choi, Y.; Jeong, S.; Vigneswaran, S. A critical review on remediation, reuse, and resource recovery from acid mine drainage. *Environ. Pollut.* **2019**, *247*, 1110–1124. [CrossRef] [PubMed]
8. Park, I.; Tabelin, C.B.; Jeon, S.; Li, X.; Seno, K.; Ito, M.; Hiroyoshi, N. A review of recent strategies for acid mine drainage prevention and mine tailings recycling. *Chemosphere* **2019**, *219*, 588–606. [CrossRef]
9. Wilfong, W.C.; Ji, T.; Duan, Y.; Shi, F.; Wang, Q.; Gray, M.L. Critical review of functionalized silica sorbent strategies for selective extraction of rare earth elements from acid mine drainage. *J. Hazard. Mater.* **2022**, *424*, 127625. [CrossRef] [PubMed]
10. Masindi, V.; Foteinis, S.; Renforth, P.; Ndiritu, J.; Maree, J.P.; Tekere, M.; Chatzisymeon, E. Challenges and avenues for acid mine drainage treatment, beneficiation, and valorisation in circular economy: A review. *Ecol. Eng.* **2022**, *183*, 106740. [CrossRef]
11. Rambabu, K.; Banat, F.; Pham, Q.M.; Ho, S.-H.; Ren, N.-Q.; Show, P.L. Biological remediation of acid mine drainage: Review of past trends and current outlook. *Environ. Sci. Ecotechnol.* **2020**, *2*, 100024. [CrossRef] [PubMed]
12. Gazea, B.; Adam, K.; Kontopoulos, A. A review of passive systems for the treatment of acid mine drainage. *Miner. Eng.* **1996**, *9*, 23–42. [CrossRef]
13. Kefeni, K.K.; Msagati, T.A.M.; Mamba, B.B. Acid mine drainage: Prevention, treatment options, and resource recovery: A review. *J. Clean. Prod.* **2017**, *151*, 475–493. [CrossRef]
14. Chen, G.; Ye, Y.; Yao, N.; Hu, N.; Zhang, J.; Huang, Y. A critical review of prevention, treatment, reuse, and resource recovery from acid mine drainage. *J. Clean. Prod.* **2021**, *329*, 129666. [CrossRef]
15. Masindi, V.; Foteinis, S.; Chatzisymeon, E. Co-treatment of acid mine drainage and municipal wastewater effluents: Emphasis on the fate and partitioning of chemical contaminants. *J. Hazard. Mater.* **2022**, *421*, 126677. [CrossRef]
16. Nkele, K.; Mpenyana-Monyatsi, L.; Masindi, V. Challenges, advances and sustainabilities on the removal and recovery of manganese from wastewater: A review. *J. Clean. Prod.* **2022**, *377*, 134152. [CrossRef]
17. Spellman, C.D.; Tasker, T.L.; Goodwill, J.E.; Strosnider, W.H.J. Potential Implications of Acid Mine Drainage and Wastewater Cotreatment on Solids Handling: A Review. *J. Environ. Eng.* **2020**, *146*, 03120010. [CrossRef]
18. Mavhungu, A.; Mbaya, R.; Masindi, V.; Foteinis, S.; Muedi, K.L.; Kortidis, I.; Chatzisymeon, E. Wastewater treatment valorisation by simultaneously removing and recovering phosphate and ammonia from municipal effluents using a mechano-thermo activated magnesite technology. *J. Environ. Manag.* **2019**, *250*, 109493. [CrossRef]
19. Mavhungu, A.; Foteinis, S.; Mbaya, R.; Masindi, V.; Kortidis, I.; Mpenyana-Monyatsi, L.; Chatzisymeon, E. Environmental sustainability of municipal wastewater treatment through struvite precipitation: Influence of operational parameters. *J. Clean. Prod.* **2021**, *285*, 124856. [CrossRef]
20. *South African National Standard (SANS) by South African Bureau of Standards (SABS) Drinking Water—Part 2: Application of SANS 241-1*; Sabs: Pretoria, South Africa, 2015.
21. Wei, X.; Viadero, R.C., Jr.; Buzby, K.M. Recovery of iron and aluminum from acid mine drainage by selective precipitation. *Environ. Eng. Sci.* **2005**, *22*, 745–755. [CrossRef]
22. Masindi, V.; Osman, M.S.; Mbhele, R.N.; Rikhotso, R. Fate of pollutants post treatment of acid mine drainage with basic oxygen furnace slag: Validation of experimental results with a geochemical model. *J. Clean. Prod.* **2018**, *172*, 2899–2909. [CrossRef]
23. Akinwekomi, V.; Maree, J.P.; Zvinowanda, C.; Masindi, V. Synthesis of magnetite from iron-rich mine water using sodium carbonate. *J. Environ. Chem. Eng.* **2017**, *5*, 2699–2707. [CrossRef]
24. Tabelin, C.B.; Corpuz, R.D.; Igarashi, T.; Villacorte-Tabelin, M.; Alorro, R.D.; Yoo, K.; Raval, S.; Ito, M.; Hiroyoshi, N. Acid mine drainage formation and arsenic mobility under strongly acidic conditions: Importance of soluble phases, iron oxyhydroxides/oxides and nature of oxidation layer on pyrite. *J. Hazard. Mater.* **2020**, *399*, 122844. [CrossRef] [PubMed]
25. Tabelin, C.B.; Veerawattananun, S.; Ito, M.; Hiroyoshi, N.; Igarashi, T. Pyrite oxidation in the presence of hematite and alumina: I. Batch leaching experiments and kinetic modeling calculations. *Sci. Total Environ.* **2017**, *580*, 687–698. [CrossRef] [PubMed]

26. Masindi, V.; Gitari, M.W.; Tutu, H.; De Beer, M. Fate of inorganic contaminants post treatment of acid mine drainage by cryptocrystalline magnesite: Complimenting experimental results with a geochemical model. *J. Environ. Chem. Eng.* **2016**, *4*, 4846–4856. [CrossRef]
27. Masindi, V.; Osman, M.S.; Shingwenyana, R. Valorization of acid mine drainage (AMD): A simplified approach to reclaim drinking water and synthesize valuable minerals—Pilot study. *J. Environ. Chem. Eng.* **2019**, *7*, 103082. [CrossRef]